Journal of Organometallic Chemistry 694 (2009) 3281–3286

Contents lists available at ScienceDirect

Journal of Organometallic Chemistry

journal homepage: www.elsevier.com/locate/jorganchem

Carbonyl rhodium(I) complexes containing (H)PNX (X = O or N) ligands deriving from natural aminoacid–amides. Synthesis, X-ray structure and spectroscopic characterization

Alessia Bacchi, Marcella Balordi, Paolo Pelagatti *, Corrado Pelizzi

Dipartimento di Chimica Generale ed Inorganica, Chimica Analitica, Chimica Fisica, University of Parma, Viale G.P. Usberti 17/A, 43100 Parma, Italy

ARTICLE INFO

Article history:
Received 22 May 2009
Received in revised form 28 May 2009
Accepted 5 June 2009
Available online 11 June 2009

Keywords:
Rhodium
PN ligands
Tridentate ligands
Amino amides
Chiral complexes

ABSTRACT

The polyfunctional (H)PNX (X = O or N) ligands **1** and **2** react with $[Rh(CO)_2Cl]_2$ to give the corresponding chloro carbonyl complexes $\{Rh[\kappa^2\text{-}(H)PN](CO)Cl\}$ (**1a** and **2a**), where the neutral ligands coordinate in a κ^2-PN bidentate fashion, the square planar coordination being completed by the CO trans to N and the chloride trans to P. In chloroform solution **1a** maintains its original structure, while **2a** partially transforms into the cationic species $\{Rh[\kappa^3\text{-}(H)PNO](CO)\}Cl$. The chloroform solutions of **1a** and **2a** react with $AgPF_6$ to give the purely cationic species $\{Rh[\kappa^3\text{-}(H)PNO](CO)\}PF_6$ ($[\mathbf{1a}]^+$ and $[\mathbf{2a}]^+$), while addition of Et_3N originates the neutral species $\{Rh[\kappa^3\text{-}PNN'](CO)\}$ (**1b** and **2b**). All the complexes have been characterized by microanalysis, IR, ^1H NMR as well as $^{31}P\{^1H\}$ NMR spectroscopy. The X-ray structures of ligand **1** and complex **1b** are also reported.

1. Introduction

The chemistry of carbonyl rhodium(I) complexes is of paramount importance both in organometallic chemistry [1] and homogeneous catalysis [2]. As our ongoing research program on the use of phosphorus-containing potentially tridentate ligands for the synthesis of organotransition metal complexes [3], here we report on the synthesis and characterization of new carbonyl rhodium(I) complexes containing chiral potentially tridentate ligands deriving from the condensation of 2-(diphenylphosphino)benzaldehyde with two different aminoacid amides, such as L-valine amide and L-valine *o*-anisidne amide. The different coordination modes of the ligands towards rhodium, such as neutral κ^2-PN, neutral κ^3-PNO and anionic κ^3-PNN′ have been investigated. The introduction of a stereogenic carbon atom in the ligand backbone opens the way to the design of enantioselective catalytic processes promoted by the title complexes.

2. Results and discussion

2.1. Synthesis of ligands *1* and *2*

The new (H)PNX (X = O, N) ligands **1** and **2** were synthesised by reacting equimolar amounts of 2-(diphenylphosphino)benzaldehyde with the appropriate amino–amide (Scheme 1). For ligand **2** the corresponding hydrochloride amino–amide was neutralized with triethylamine prior to condensation. The reactions were conducted in $MeOH/CH_2Cl_2$ at 50 °C, isolating white (**1**) or light yellow (**2**) solids in good yields. The completion of the condensation reaction was checked by TLC (SiO_2, EtOAc/n-hexane) or by liquid film IR spectroscopy.

In the IR spectra the stretching bands of the amide group are centered at 1685 and 1679 cm^{-1} for **1** and **2**, respectively. The stretching of the amide N–H bonds generates large bands in the region 3200–3400 cm^{-1}. The ^1H NMR spectra of the ligands recorded in CD_2Cl_2 show the imine signal in the region 8–9 ppm. Only in the case of **1** the coupling with the phosphorus nucleus is evident, giving rise to a doublet with a $^4J_{HP}$ = 5 Hz, while in the spectra of **2** the same signal gives rise to a broad singlet. The amide protons of **2** give rise to two distinct broad singlets at 6.65 and 5.33 ppm. The amide proton of **1**, where the nitrogen is bound to an *o*-An ring, resonates to lower fields, giving rise to a singlet at 9.33 ppm, symptom of a high acidic character. The $^{31}P\{^1H\}$ NMR spectra of the ligands recorded in deuterated dichloromethane show a singlet at −13.5 and −10.6 ppm for **1** and **2**, respectively. Ligands **1** and **2** are stable in the solid state towards oxidation of the phosphine moiety, as evidenced by $^{31}P\{^1H\}$ NMR spectroscopy. Traces of oxidation become instead visible leaving the solutions of the ligands in plain air for several days, as indicated by the appearance of a singlet at about 33 ppm in the $^{31}P\{^1H\}$ NMR spectra. Formation of the corresponding phosphine oxides can be avoided on storing the

* Corresponding author. Fax: +39 0521 905557.
E-mail address: paolo.pelagatti@unipr.it (P. Pelagatti).

0022-328X/$ - see front matter © 2009 Elsevier B.V. All rights reserved.
doi:10.1016/j.jorganchem.2009.06.008

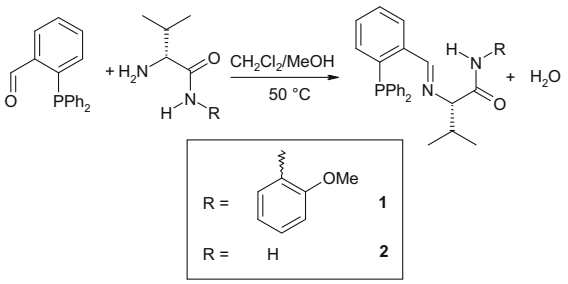

Scheme 1. General scheme for the ligands **1** and **2**.

solutions under nitrogen. From a refrigerated methanol solution of **1**, crystals suitable for X-ray analysis were collected. The solid structure of the ligand is reported in Fig. 1 along with the labeling scheme.

The molecular structure of **1** is potentially highly flexible, due to the many conformational degrees of freedom around the single bonds along the molecular skeleton. Namely, six main torsion angles can be evidenced to best represent the overall molecular folding, indicated as ***T1***–***T6*** in Fig. 1, besides the potential source of *E*/*Z* isomerism represented by the C=N double bond (the rotation of the diphenylphosphine aromatic groups is not considered as significant). Table 1 lists the values of these torsion angles observed in the solid state for the molecular structure of the free ligand **1**.

It can be evidenced that, while the two potential nitrogen donor sites N1 and N2 are already correctly prepositioned for creating a virtual chelation site, the phosphorus donor points away, due to a inconvenient orientation of ***T5***. Actually, a closer approach of P1 to N1 and N2 in the potential coordination site is not to be excluded by mere steric considerations, since cases with a similar pattern of intramolecular NH···P···N distances as well as examples of intramolecular linear NH···P contacts between a NH and a phosphorous lone pair have been already characterized in the literature [4]. Nevertheless, the extended folding adopted by free **1** is evidently electrostatically stabilized by the local arrangement of O2 and N2 around N1–H, that would be disrupted by the entrance of the phosphine group in the site.

2.2. Synthesis of the rhodium complexes *1a*–*2a*

$[Rh(CO)_2Cl]_2$ reacts in diethyl ether at room temperature with a twofold excess of ligands **1** and **2** giving rise to the fast precipitation of orange solids (Scheme 2).

The elemental analyses of the isolated products are in agreement with the general formula {Rh[(H)PNX](CO)Cl}. The IR spectra of the solids show an intense carbonyl stretching band centered at 2003 and 1990 cm^{-1}, for **1a** and **2a,** respectively, while the ν(C=O) band of the amide group is centered in both cases at values very close to those of the free ligands, thus indicating its exclusion from coordination. The stretchings of the N–H bonds give rise to an intense absorption at 3258 cm^{-1} for **1a** and large bands in the region 3200–3400 cm^{-1} for **2a**. The ^1H NMR spectra recorded in $CDCl_3$ show the presence of the amide protons with a very broad singlet at 9.86 ppm for **1a**, while for **2a** only a proton is visible as a broad singlet at 7.8 ppm. In order to reduce the chemical exchange the spectrum of **2a** was recorded also in deuterated dmso, where the amide protons are both visible as broad singlets at 9.49 and 9.13 ppm, respectively. The $^{31}P\{^1H\}$ NMR spectrum of **1a** recorded in $CDCl_3$ shows a doublet centered at 45 ppm with a $^1J_{Rh-P}$ = 142 Hz. Diversely, the $^{31}P\{^1H\}$ NMR spectrum of **2a** shows two doublets, centered at 52.5 and 43.5 ppm, with $^1J_{Rh-P}$ = 161 and 129.5 Hz, respectively. The two doublets are in a 1:0.3 ratio in favor of the more deshielded signal. The addition of a slight excess of $AgPF_6$ to the chloroform solutions of **1a** and **2a** leads to the rapid precipitation of AgCl. The remaining solutions show a unique doublet centered at 53 ppm with a $^1J_{Rh-P}$ = 172 Hz belonging to the purely cationic complexes {Rh[(H)PNO](CO)}PF_6 ([**1a**]PF_6 and

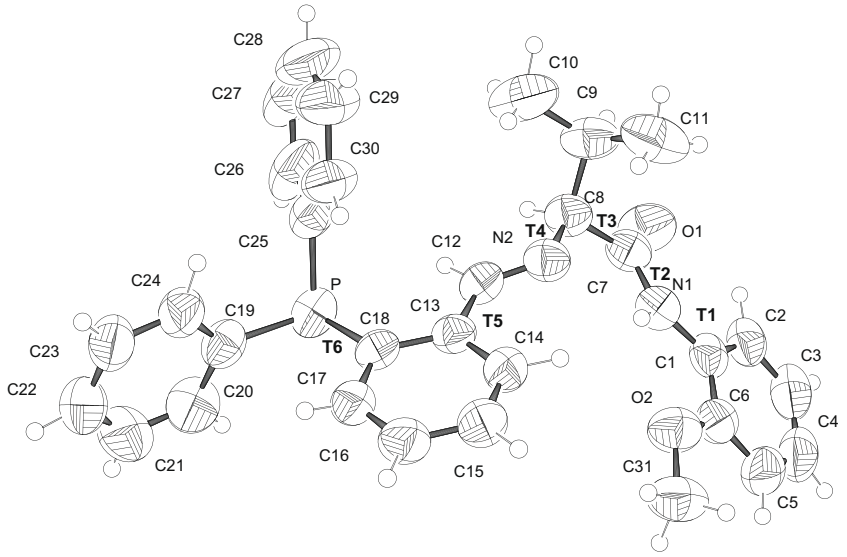

Fig. 1. Perspective view of the molecular structure of **1**, with thermal ellipsoids at the 50% probability level. Torsion angles discussed in the text are indicated as ***T1***–***T6***.

Table 1
Comparison of the most relevant torsion angles (°) defining the molecular conformation of **1** and **1b**.

	T1 (C6–C1–N1–C7)	***T2*** (C1–N1–C7–C8)	***T3*** (N1–C7–C8–N2)	***T4*** (C7–C8–N2–C12)	***T5*** (N2–C12–C13–C18)	***T6*** (C13–C18–P1–C19)
1	−165	173	−9	−121	170	−176
1b	60	−177	−36	−134	16	−171

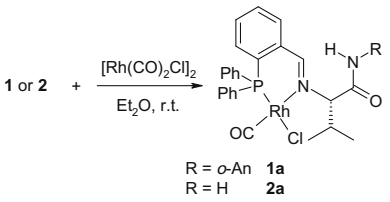

Scheme 2. General scheme for the synthesis of the chloro–carbonyl complexes **1a** and **2a**.

[**2a**]PF_6 in Scheme 3); in both cases the PF_6 anion resonates as a septuplet at −145 ppm. Chloroform solutions of **1a** and **2a** have been analyzed by MS-spectrometry by means of a DEP probe (see Section 4). The mass spectrum of **1a** shows an intense signal at m/z = 596 corresponding to the loss of HCl and CO, while a second signal at m/z = 581 originates from the successive loss of the methyl group from the anisidine moiety. The mass spectrum of **2a** shows a signal at m/z = 518 corresponding to the loss of HCl, while a second, less intense, signal at m/z = 475 originates from the successive loss of the carbonyl ligand.

Although it has not been possible to grow X-ray quality crystals for the complexes **1a** and **2a**, their structures in solution can be inferred by the aforementioned characterization data. The most likely structure for chloro–carbonyl complexes of Rh(I) with phosphine–imine ligands is represented by the square planar coordination, with the four positions occupied by the P and N donors of ligands **1** and **2** and by the CO and chloride ligands trans to N and P, respectively. This represents the most thermodynamic stable ligand disposition around the metal. The microanalysis and IR data indicate that this is the case for both complexes in the solid state [5]. In solution, however, two different situations are found. With **1a** only one species is observed, while with **2a** there is the coexistence of two different species. The square planar geometry is expected to create a steric repulsion between the isopropyl group of the tridentate ligands with the chloride one, repulsion which could be removed by changing the coordination mode of the chelating from κ^2-PN to κ^3-PNO (Scheme 3). For neutral amide ligands the coordination through oxygen is certainly more favoured than that through nitrogen [6]. This change in the hapticity of the ligand is not observed with **1a** which in fact shows a unique doublet at 45 ppm in its $^{31}P\{^1H\}$ NMR spectrum. This signal is then assigned to the neutral species {Rh[κ^2-(H)PN](CO)Cl}. For complex **2a** instead, the doublet at 43.5 ppm is attributed to the neutral species {Rh[κ^2-(H)PN](CO)Cl} (**2a**), while the doublet at 52.5 ppm is attributed to the cationic species {Rh[κ^3-(H)PNO](CO)}Cl ([2a]Cl in Scheme 3), where **2** behaves as a neutral tridentate PNO ligand.

The replacement of an amide proton with a *o*-An function seems then to block the rotation around the C*—C(O)N bond of the ligand, rotation necessary in order to pass from **1a** to [**1a**]$^+$, likely because of steric reasons. This rotation occurs only after removal of the halogen ligand by a halogen scavenger or a base (*vide infra*).

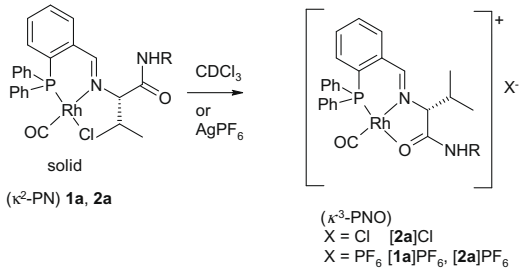

Scheme 3. From κ^2-PN to κ^3-PNO hapticity.

In order to test the possibility of forcing the ligands to coordinate rhodium in an anionic tridentate fashion [7], dichloromethane solutions of the complexes **1a** and **2a** were treated with an excess of triethylamine at room temperature. After removal of the ammonium salt the neutral carbonyl complexes **1b** and **2b** were isolated (Scheme 4).

These are light orange solids, stable in the solid state as well as in solution. The deprotonation of the ligands forces the amide nitrogen to coordinate rhodium [8], and this provokes a shift of the C=O amide stretching band to lower frequencies, from 1686 to 1606 cm^{-1} for **1b** and from 1666 to 1629 cm^{-1} for **2b**, respectively [8,9]. The deprotonation of the amide function is evident in the ^1H NMR spectra of the complexes. For **1b** the spectrum recorded in $CDCl_3$ does not show any acidic signal, while the spectrum of **2b** recorded in dmso-d_6 shows only a broad singlet at 6.10 ppm, corresponding to the residual NH function. The carbonyl stretching region contains a unique intense band centered at 1981 and 1982 cm^{-1} for **1b** and **2b**, respectively. The shift to lower frequencies of the carbonyl group with respect to the precursors is attributable to the higher electron density that the anionic tridentate ligands place on the metal. This provokes a higher metal to ligand back-donation which reduces the bond order of the CO. The $^{31}P\{^1H\}$ NMR spectra of **1b** recorded in $CDCl_3$ shows a singlet at 45 ppm, with a $^1J_{RhP}$ = 143 Hz, values very similar to those found for **1a** in the same solvent. This is not a totally unexpected behavior, which has already been observed by us with chloro–carbonyl rhodium(I) complexes containing tridentate acyl-hydrazones on passing from a κ^2-(H)PN coordination to a κ^3-PNO one [3c]. The $^{31}P\{^1H\}$ NMR spectrum of **2b** recorded in dmso-d_6 shows a doublet at 47.7 ppm with a $^1J_{Rh-P}$ = 133 Hz.

The solid structure of **1b** has been definitively established by X-ray diffraction analysis on a single crystal grown by slow diffusion of diethyl ether into a dichloromethane solution of the complex.

The crystalline structure of **1b** is reported in Fig. 2.

Upon complexation, **1** is deprotonated and changes remarkably its conformation in order to adopt a tridentate PNN′ chelation mode in **1b**, with a CO ligand *trans* to the imine nitrogen completing a square planar coordination around rhodium. The major conformational alterations due to coordination are evidenced by the comparison of torsion angles along the molecular backbones of **1** and **1b** listed in Table 2, and involve a 180° rotation of the triphenylphosphino group around ***T5*** aimed to bring the phosphorus donor in the chelation site, and a parallel rotation by 100° of the *o*-methoxy-phenyl ring around ***T1*** in order to bring the methoxy substituent away from the coordination core. Two remarkably puckered chelation systems are thus created, namely a six-membered ring comprising P1 and N2, presenting an envelope conformation with the metal deviating by 0.92 Å from the mean plane defined by P1, C18, C12, C13, N2, and a five-membered ring containing N1 and N2, presenting a twisted conformation with C7 and C8 displaced from the plane defined by Rh1, N1 and N2, in a λ absolute configuration. The combination of the deformations of the two chelation rings fused at the common Rh1–N2 bond influences the overall geometry of the coordination site of **1b**, that can be regarded as a butterfly configuration hinged on the P1–N2

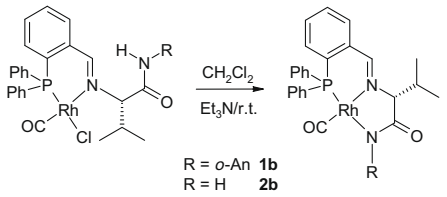

Scheme 4. Synthesis of the carbonyl complexes **1b** and **2b**.

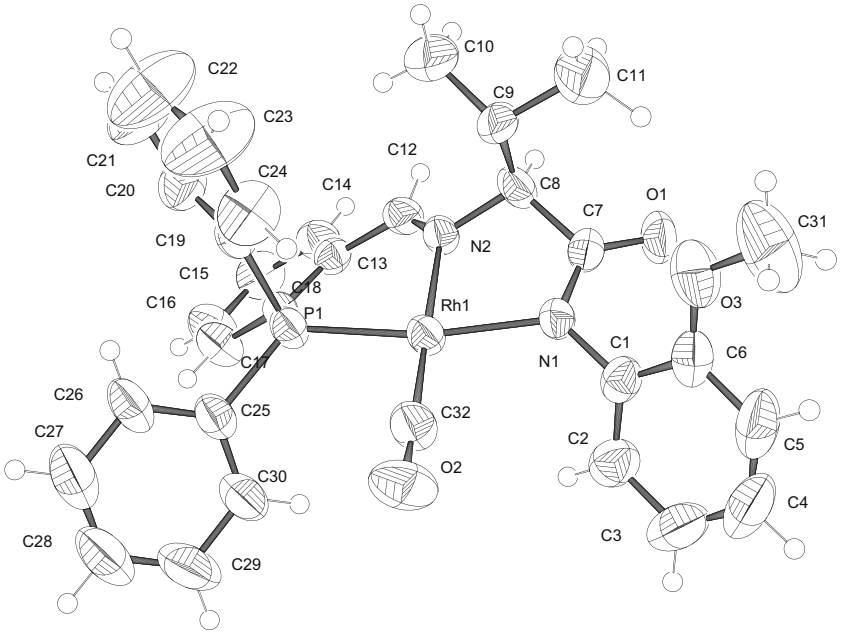

Fig. 2. Perspective view of the molecular structure of **1b**, with thermal ellipsoids at the 50% probability level. Relevant coordination parameters with e.s.d.'s in parentheses (Å,°): Rh1–P1 2.207(1), Rh1–N1 2.061(3), Rh1–N2 2.062(3), Rh1–C32 1.811(4); P1–Rh1–N1 167.42(9), P1–Rh1–N2 87.32(9), P1–Rh1–C32 93.8(1), N1–Rh1–N2 80.1(1), N1–Rh1–C32 98.8(2), N2–Rh1–C32 177.8(2).

Table 2
Crystal data and structure refinement for **1** and **1b**.

	1	**1b**
Empirical formula	$C_{31}H_{31}N_2O_2P$	$C_{32}H_{30}N_2O_3PRh$
Formula weight	494.55	624.46
Temperature (K)	293(2)	293(2)
Wavelength (Å)	1.54178	0.71073
Crystal system	orthorhombic	orthorhombic
Space group	$P\,2_1\,2_1\,2_1$	$P\,2_1\,2_1\,2_1$
Unit cell dimensions (Å)	a = 26.112(8)	a = 11.8359(7)
	b = 15.256(6)	b = 15.3258(9)
	c = 7.002(2)	c = 16.491(1)
Volume (Å^3)	2789.3(16)	2991.4(3)
Z	4	4
Density (calculated) (Mg/m^3)	1.178	1.387
Absorption coefficient (mm^{-1})	1.096	0.658
F(0 0 0)	1048	1280
θ range for data collection (°)	3.36–70.81	1.81–23.29
Reflections collected	10 639	24 726
Independent reflections	5335 [R_{int} = 0.0305]	4304 [R_{int} = 0.0546]
Data/restraints/parameters	5335/0/449	4304/0/406
Goodness-of-fit on F^2	0.942	0.861
Final R indices [$I>2\sigma(I)$]	R_1 = 0.0412,	R_1 = 0.0277,
	wR_2 = 0.0800	wR_2 = 0.0443
R indices (all data)	R_1 = 0.0713,	R_1 = 0.0402,
	wR_2 = 0.0910	wR_2 = 0.0466
Absolute structure parameters	−0.03(2)	0.02(2)
Largest ΔF residuals (e Å^{-3})	0.100/−0.179	0.355 and −0.177

direction. The two planes constituting the butterfly wings consist respectively of (Rh1, C32, O2, N1, C7, C8, N2, P1) and (N2, P1, C12–C18), and make a dihedral angle of 39°.

3. Conclusions

In the present work we have shown the synthesis and characterization of two new chiral polyfunctional ligands obtained by condensation of 2-(diphenylphosphino)benzaldehyde with two different types of amino acid amides (ligands **1** and **2**). These give rise to square planar carbonyl rhodium(I) complexes where the chiral ligands behave as neutral κ^2-(H)PN chelatings (**1a** and **2a**). In chloroform solution this behavior is retained with **1**, while **2** tends to involve also the amide function in a neutral κ^3-(H)PNO fashion. A neutral tridentate behavior is observed upon addition of $AgPF_6$, leading to the cationic species [**1a**]$^+$ and [**2a**]$^+$. The addition of an excess of triethylamine to chloroform solutions of **1a** and **2a** leads to the clean deprotonation of the amide function with isolation of neutral carbonyl complexes where both ligands exert a anionic κ^3-PNN′ behavior (**1b** and **2b**).

The study of the complexes as potential chiral catalysts is currently under investigation in our laboratory.

4. Experimental

4.1. General methods

All reactions were performed under an atmosphere of dry nitrogen, employing standard Schlenk techniques. Solvents were dried prior to use and stored over molecular sieves and under nitrogen. Elemental analysis (C, H, N) were performed by using a Carlo Erba Mod. EA 1108 apparatus. Infrared spectra were recorded with a Nicolet 5PCFT-IR spectrophotometer in the range 4000–400 cm^{-1} by using KBr disks. ^{1}H NMR spectra were obtained at 300 K on a Bruker 300 FT spectrometer, while ^{31}P{^{1}H}-NMR spectra were collected on a Bruker AMX 400 FT by using H_3PO_4 85% as external standard. The FAB(+)-MS spectra were collected by an EVG Autospec M, using *m*-nitrobenzyl alcohol as matrix. The EI(+)-MS spectra were collected with a DSQ-II Thermo Scientific mass-spectrometer equipped with a single quadrupole mass-analyzer, by means of a direct exposure probe (DEP) mounting a rhenium filament. The analyses were conducted applying a ramp of 100 mA/s from 30 to 1000 mA, with an electron potential of 70 eV. The enantiomerically pure Boc-protected amino acids and the commercially available amino acid amides have been used as received without further purifications. *N*-(*tert*-Butoxycarbonyl)-(L)-valyne *o*-anisidine amide was synthesised as already reported [8b]. 2-(diphenylphosphino)benzaldehyde was purchased by Aldrich and purified by chromatographic column prior condensation. [$Rh_2(CO)_4Cl_2$] was purchased by Aldrich.

4.2. Synthesis of the ligands

4.2.1. Ligand **1**

Five hundred and seventy milligrams (1.8 mmol) of *N*-(*tert*-butoxycarbonyl)-L-valyne *o*-anisidine amide were dissolved in 15 ml of dichloromethane. The resulting solution was treated with 10 equivalents of trifluoroacetic acid and stirred for two hours at room temperature. The solvent was then removed under vacuum and the residue dissolved in 10 ml of a 0.2 M KOH solution and extracted with 40 ml of dichloromethane. The solution was concentrated under vacuum before adding 510 mg (1.8 mmol) of 2-(diphenylphosphino)benzaldehyde and anhydrous Na_2SO_4. The yellow solution was heated at 50 °C for 12 h under stirring, then filtered and dried under vacuum. The resulting whitish sticky residue was dissolved in methanol and the solution refrigerated at −18 °C obtaining a white powder. From a methanol solution of the ligand refrigerated at −18 °C crystals suitable for X-ray analysis were collected. Yield: 560 mg (63%). M.p.: 138.4–139.1 °C. Anal. Calc. for $C_{31}H_{31}N_2O_2P$: C, 75.30; H, 6.28; N, 5.67. Found: C, 75.21; H, 6.33; N, 5.49%. ^{1}H NMR (CD_2Cl_2): δ 9.33 (s, 1H, NH), 8.86 (d, 1H, CH=N, $^4J_{HP}$ = 5 Hz), 8.34 (dd, 1H, An, $^3J_{HH}$ = 7.8 Hz, $^4J_{HH}$ = 1.3 Hz), 8.18 (m, 1H, Ph), 7.49 (t, 1H, Ph, $^3J_{HH}$ = 7 Hz), 7.42–7.26 (m, 11H, Ph), 7.07 (td, 1H, An, $^3J_{HH}$ = 7.7 Hz, $^4J_{HH}$ = 1.5 Hz), 6.96 (m, 3H, Ph + An) 3.90 (s, 3H, OCH_3), 3.62 (d, 1H, C*H, $^3J_{HH}$ = 4.5 Hz), 2.19 (m, 1H, C*H*(CH_3)$_2$), 0.73 (d, 3H, CH(C*H*$_3$)$_2$, $^3J_{HH}$ = 5.9 Hz), 0.68 (d, 3H, CH(C*H*$_3$)$_2$, $^3J_{HH}$ = 5.9 Hz). ^{31}P{^{1}H}-NMR (CD_2Cl_2): δ-13.5 (s). IR: 3324 (NH), 1685 (C=O). FAB(+)-MS: *m*/*z* = 495 [**1**+H$^+$]$^+$.

4.2.2. Ligand **2**

Two hundred and sixty milligrams (1.7 mmol) of L-valineamide hydrochloride were dissolved in 15 ml of methanol and 0.28 ml (1.2 mmol) of triethylamine were added. After 2 h of stirring at room temperature 490 mg (1.7 mmole) of 2-(diphenylphosphino)benzaldehyde dissolved in 10 ml of dichloromethane were added, and the solution was stirred at 50 °C for 24 h in the presence of anhydrous Na_2SO_4. After filtration, the solvent was removed under vacuum and the residue dissolved in toluene, passed through a silica pad and the resulting clear solution dried under vacuum. The solid is again dissolved in methanol and the solution refrigerated at −18 °C, obtaining a yellow powder. Yield: 460 mg (67%). M.p.: 106.4–107.1 °C. Anal. Calc. for $C_{24}H_{25}N_2OP$: C, 74.23; H, 6.44; N, 7.22. Found: C, 74.08; H, 6.80; N, 6.52%. ^{1}H NMR (CD_2Cl_2): δ 8.47 (sbr, 1H, CH=N), 7.80 (m, 1H, Ph), 7.49 (t, 1H, Ph, $^3J_{HH}$ = 7.5 Hz), 7.37–7.27 (m, 7H, Ph), 7.26–7.19 (m, 4H, Ph), 6.94 (m, 1H, Ph), 6.65 (sbr, 1H, NH_2), 5.33 (sbr, 1H, NH_2), 3.53 (d, 1H, C*H, $^3J_{HH}$ = 4.3 Hz), 2.12 (m, 1H, C*H*(CH_3)$_2$), 0.74 (d, 3H, CH_3, $^3J_{HH}$ = 6.8 Hz), 0.63 (d, 3H, CH_3, $^3J_{HH}$ = 6.8 Hz). ^{31}P{^{1}H}-NMR (CD_2Cl_2): δ-10.6 (s). IR: 3400–3275 (NH_2), 1679 (C=O). FAB(+)-MS: *m*/*z* = 389 [**2**+H$^+$]$^+$.

4.3. Synthesis of the complexes

4.3.1. Complexes {Rh[κ^2-(H)PN](CO)Cl} (**1a**–**2a**)

*4.3.1.1. Complex **1a**.* One hundred and fifty milligrams (0.3 mmol) of **1** were dissolved in 20 ml of diethyl ether and 60 mg (0.15 mmol) of $[Rh(CO_2)Cl]_2$ were added. The orange solution was stirred at room temperature for 5 h. The shiny orange solid formed was filtered off, washed with diethyl ether and *n*-hexane and finally dried under vacuum. Yield: 160 mg (80%). M.p.: 179 °C (dec.). Anal. Calc. for $C_{32}H_{31}ClN_2O_3PRh$: C, 58.18; H, 4.97; N, 4.24. Found: C, 58.42; H, 4.71; N, 4.33%. ^{1}H NMR ($CDCl_3$): δ 9.86 (sbr, 1H, NH), 8.69 (s, 1H, C(H)=N), 8.18 (br, 1H, An), 7.62–6.87 (m, 20H, Ph + An), 5.64 (d, 1H, C*H, $^3J_{HH}$ = 9.9 Hz), 3.94 (s, 3H, OCH_3), 2.17 (m, 1H, C*H*(CH_3)$_2$), 0.94 (d, 3H, CH(C*H*$_3$)$_2$, $^3J_{HH}$ = 5.9 Hz), 0.52 (d, 3H, CH(C*H*$_3$)$_2$, $^3J_{HH}$ = 5.9 Hz). ^{31}P{^{1}H}-NMR (CD_2Cl_2): δ 45.0 (d, $^1J_{RhP}$ = 142 Hz). IR: 3258 (NH), 2005 (C≡O), 1685 (C=O). EI(+)-MS (DEP): *m*/*z* = 596 [**1a**-HCl–CO]$^+$, 581 [596-CH_3]$^+$.

*4.3.1.2. Complex **2a**.* As for **1** but starting from **2**. Yield: 180 mg (72%). M.p.: 210 °C (dec.). Anal. Calc. for $C_{25}H_{25}ClN_2O_2PRh\cdot 1/2H_2O$: C, 58.28; H, 4.44; N, 4.97. Found: C, 53.03; H, 4.48; N, 4.68%. ^{1}H NMR ($CDCl_3$): δ 8.52 (s, 1H, C(H)=N), 7.80 (sbr, 1H, NH), 7.70-7.42 (m, 13H, Ph), 7.04 (tbr, 1H, Ph), 5.32 (d, 1H, C*H, $^3J_{HH}$ = 9.9 Hz), 2.29 (m, 1H, C*H*(CH_3)$_2$), 1.88 (sbr, 1H, NH), 0.92 (d, 3H, CH(C*H*$_3$)$_2$, $^3J_{HH}$ = 5.9 Hz), 0.62 (d, 3H, CH(C*H*$_3$)$_2$, $^3J_{HH}$ = 5.9 Hz). ^{31}P{^{1}H}-NMR ($CDCl_3$): major signal: δ 52.5 (d, $^1J_{RhP}$ = 161 Hz); minor signal: δ 43.5 (d, $^1J_{RhP}$ = 129.5 Hz). IR: 3250 (NH), 2076 (C≡O), 1666 (C=O). EI(+)-MS (DEP): *m*/*z* = 518 [**2a**-HCl]$^+$, 475 [518-CO]$^+$.

4.3.2. Synthesis of the complexes {Rh[κ^3-PNN′](CO)} (**1b**–**2b**)

*4.3.2.1. Complex **1b**.* Hundred milligrams of complex **1a** (0.150 mmol) were dissolved in 15 ml of dichloromethane and 5 equivalents of Et_3N were added to the resulting solution. After a prolonged stirring at room temperature (12 h) the solvent was removed under vacuum and the resulting solid was treated with toluene. After filtration over a plug of celite the solution was concentrated under vacuum, treated with n-hexane and refrigerated at −18 °C. A light orange powder was filtered off and washed with n-hexane and finally dried under vacuum. Yield: 90 mg (56%). M.p.: 167.6–168.1 °C. Anal. Calc. for $C_{32}H_{30}N_2O_3PRh$: C, 61.53; H, 4.81; N, 4.49. Found: C, 60.83; H, 4.92; N, 4.32%. ^{1}H NMR (CD_2Cl_2): δ 7.87 (s, 1H, C(H)=N), 7.61–6.87 (m, 18 H, Ph), 3.99 (d, 1H, C*H, $^3J_{HH}$ = 3.9 Hz), 3.87 (s, 3H, OCH_3), 2.47 (mbr, 1H, C*H*(CH_3)$_2$), 0.94 (d, 3H, CH(C*H*$_3$)$_2$, $^3J_{HH}$ = 5.9 Hz), 0.75 (d, 3H, CH(C*H*$_3$)$_2$, $^3J_{HH}$ = 5.9 Hz). ^{31}P{^{1}H} NMR (CD_2Cl_2): δ 45.0 (d, $^1J_{RhP}$ = 143 Hz). IR: 1983 ν(C≡O), 1606 ν(C=O), 1454 ν(P–Ph). By slow diffusion of diethyl ether into a dichloromethane solution of **1b**, X-ray quality crystals were collected.

*4.3.2.2. Complex **2b**.* As for **1b** but starting from **2a**. Yield: 69 mg (77%). M.p.: 112.4–113 °C. Anal. Calc. for $C_{25}H_{24}N_2O_2PRh$: C, 57.93; H, 4.63; N, 5.40. Found: C, 57.51; H, 4.58; N, 5.22%. ^{1}H NMR (dmso-d_6): δ 8.36 (s, 1H, C(H)=N), 7.80–7.06 (m, 14H, Ph), 6.10 (s, 1H, NH), 3.73 (d, 1H, C*H, $^3J_{HH}$ = 4.9 Hz), 2.18 (m, 1H, C*H*(CH_3)$_2$), 0.77 (d, 3H, CH(C*H*$_3$)$_2$, $^3J_{HH}$ = 5.9 Hz), 0.55 (d, 3H, CH(C*H*$_3$)$_2$, $^3J_{HH}$ = 5.9 Hz). ^{31}P{^{1}H} NMR (dmso-d_6): δ 47.7 (d, $^1J_{RhP}$ = 133 Hz). IR: 1983 ν(C≡O); 1629 ν(C=O); 1435 ν(P–Ph).

4.4. X-ray diffraction analysis

CuKα radiation (λ = 1.54178 Å), *T* = 293 K, on a Siemens AED diffractometer equipped with scintillation detector was employed for **1**, while MoKα radiation (λ = 0.71073 Å), *T* = 293 K, on a SMART AXS 1000 diffractometer equipped with CCD detector was used for compound **1b**. Lorentz, polarization, and absorption corrections were applied [10]. Structures were solved by direct methods using SIR97 [11] and refined by full-matrix least-squares on all F^2 using SHELXL97 [12] implemented in the WINGX package [13]. Hydrogen atoms were partly located on Fourier difference maps and refined isotropically, partly introduced in calculated positions. Anisotropic displacement parameters were refined for all non-hydrogen atoms. Final geometries have been analyzed with SHELXL97 [12] and PARST97 [14], and extensive use was made of the Cambridge Crystallographic Data Centre packages [15]. Table 2 summarizes crystal data and structure determination results.

Supplementary material

CCDC 733396 and 733397 contain the supplementary crystallographic data for this paper. These data can be obtained free of

charge from The Cambridge Crystallographic Data Centre via www.ccdc.cam.ac.uk/data_request/cif.

Acknowledgments

The authors thank Prof. María C. Rodríguez Argüelles (University of Vigo, Spain) for the FAB-MS analyses, and Centro Interdipartimentale "G. Casnati" of the University of Parma for the instrument facilities.

References

[1] A. Yamamoto, Organotransition Metal Chemistry: Fundamental Concepts and Applications, John Wiley and Sons, Inc., New York, 1986.
[2] (a) G.W. Parshall, S.D. Ittel, Homogeneous Catalysis: The Application and Chemistry of Catalysis by Soluble Transition Metal Complexes, second ed., John Wiley and Sons., Inc., New York, 1992;
(b) J.G. de Vrieze, C.J. Elsevier, Handbook of Homogeneous Hydrogenation, Wiley-VCH, Weinheim, 2007.
[3] (a) P. Pelagatti, A. Bacchi, M. Balordi, S. Bolaño, F. Calbiani, L. Elviri, L. Gonsalvi, C. Pelizzi, M. Peruzzini, D. Rogolino, Eur. J. Inorg. Chem. (2006) 2422–2436;
(b) P. Pelagatti, A. Bacchi, M. Balordi, A. Caneschi, M. Giannetto, C. Pelizzi, L. Gonsalvi, M. Peruzzini, F. Ugozzoli, Eur. J. Inorg. Chem. (2007) 162–171;
(c) P. Pelagatti, A. Bacchi, C. Bobbio, M. Carcelli, M. Costa, C. Pelizzi, C. Vivorio, Organometallics 19 (2000) 5440–5446;
(d) P. Pelagatti, A. Bacchi, C. Bobbio, M. Carcelli, M. Costa, A. Fochi, C. Pelizzi, J. Chem. Soc., Dalton Trans. (2002) 1820–1825;
(e) P. Pelagatti, A. Bacchi, M. Carcelli, M. Costa, H.-W. Frühauf, K. Goubitz, C. Pelizzi, M. Triclistri, K. Vrieze, Eur. J. Inorg. Chem. (2002) 439–446.
[4] (a) Y. Matano, M. Nakashima, T. Nakabuchi, H. Imahori, S. Fujishige, H. Nakano, Org. Lett. 10 (2002) 553–556;
(b) S. Burger, B. Therrien, G. Suss-Fink, Inorg. Chim. Acta 357 (2004) 1213–1218.
[5] (a) M.P. Anderson, A.L. Casalnuovo, B.J. Johnson, B.M. Mattson, A.M. Mueting, L.H. Pignolet, Inorg. Chem. 27 (1988) 1649–1658;
(b) J. Best, J.M. Wilson, H. Adams, L. Gonsalvi, M. Peruzzini, A. Haynes, Organometallics 26 (2007) 1960–1965.
[6] (a) J.P. Costes, J.P. Laurent, Inorg. Chem. 27 (1988) 3235–3237;
(b) A. Bacchi, P. Pelagatti, C. Pelizzi, D. Rogolino, J. Organomet. Chem. 694 (2009) 3200–3211.
[7] (a) J.A. Fuentes, M.L. Clarke, A.M.Z. Slawin, New J. Chem. 32 (2008) 689–693;
(b) M.R.J. Elsegood, A.J. Lake, M.B. Smith, Eur. J. Inorg. Chem. (2009) 1068–1078.
[8] (a) P. Pelagatti, A. Bacchi, F. Calbiani, M. Carcelli, L. Elviri, C. Pelizzi, D. Rogolino, J. Organomet. Chem. 690 (2005) 4602–4610;
(b) P. Pelagatti, M. Carcelli, F. Calbiani, C. Cassi, L. Elviri, C. Pelizzi, U. Rizzotti, D. Rogolino, Organometallics 24 (2005) 5836–5844.
[9] (a) R. Krämer, M. Maurus, R. Bergs, K. Polborn, K. Sünkel, B. Wagner, W. Beck, Chem. Ber. 126 (1996) 1969–1980;
(b) W. Hoffmüller, K. Polborn, J. Knizek, H. Nöth, W. Beck, Z. Anorg. Allg. Chem. 623 (1997) 1903–1911.
[10] (a) SAINT: SAX, Area Detector Integration, Siemens Analytical Instruments INC., Madison, Wisconsin, USA;
(b) G. Sheldrick, SADABS: Siemens Area Detector Absorption Correction Software, University of Goettingen, Germany, 1996;
(c) SMART for WNT/2000 version 5.622, Smart Software Reference Manual, Bruker Advanced X-ray Solution, Inc., Madison, WI, 2001.
[11] A. Altomare, M.C. Burla, M. Cavalli, G. Cascarano, C. Giacovazzo, A. Gagliardi, A.G. Moliterni, G. Polidori, R. Spagna, Sir97: A New Program For Solving And Refining Crystal Structures, Istituto di Ricerca per lo Sviluppo di Metodologie Cristallografiche, CNR, Bari, 1997.
[12] G. Sheldrick, SHELXl97. Program for structure refinement. University of Goettingen, Germany, 1997.
[13] L.J. Farrugia, J. Appl. Cryst. 32 (1999) 837–838.
[14] M. Nardelli, J. Appl. Cryst. 28 (1995) 659.
[15] (a) F.H. Allen, O. Kennard, R. Taylor, Acc. Chem. Res. 16 (1983) 146–153;
(b) I.J. Bruno, J.C. Cole, P.R. Edgington, M. Kessler, C.F. Macrae, P. McCabe, J. Pearson, R. Taylor, Acta Crystallogr. B58 (2002) 389–397.